



In vitro biological, catalytic, and DFT studies of some iron(III) N-ligated complexes

Ahmed K. Hijazi¹ · Ziyad A. Taha¹ · Taher S. Ababneh² · Heba M. Alshare¹ · Nezar Al-Bataineh³ · Waleed M. Al-Momani⁴ · Abdulaziz M. Ajlouni¹

Received: 13 May 2019 / Accepted: 22 November 2019
© Institute of Chemistry, Slovak Academy of Sciences 2019

Abstract

Fe(III) complexes, $[\text{Fe}(\text{CH}_3\text{CN})_6][\text{X}]_3$ and $[\text{Fe}(\text{CH}_3\text{CH}_2\text{CN})_6][\text{X}]_3$ (where X: counter anion = $\text{B}\{\text{C}_6\text{H}_3(\text{m}-\text{CF}_3)_2\}_4^-$ and $\text{B}(\text{C}_6\text{F}_5)_4^-$) have been synthesized by the reaction of FeCl_3 with $\text{Ag}[\text{B}(\text{X})_4]$. Full characterization for the complexes has been done in solution and in the solid state. The complexes are obtained in good yields and are moderately sensitive to air. All complexes have been used as catalysts for aniline oxidation with yields up to 62%, in which azobenzene is the only product. Furthermore, they exhibit good antimicrobial properties. The Fe(III) complexes molecular geometries have been studied using DFT calculations at the B3LYP/6-31G(d) and B3LYP/6-31+G(d, p) levels of theory and obtained results are in agreement with the experimental data.

Keywords Catalysis · N-ligands · Aniline oxidation · Antimicrobial · Weakly coordinated anions · DFT

Introduction

First transition metal series complexes with a formula of $[\text{M}^{\text{II}}(\text{NCR})_{4-6}][\text{X}]_2$ (M = first transition metal series; R = C_6H_5 , CH_3CH_2 , CH_3 ; X = counter anion) with their dimeric congeners are long known by, Hathaway and Holah (1964), Angerman and Jordan (1969), Johnson et al. (1978), Thomas et al. (1986), Rapaport et al. (1988), Thomas and Sen (1989), Henriques et al. (1998), Buschmann and Miller (1998) and (2002), Cotton and Kühn (1996), Liang et al. (2002), Rach and Kühn (2009). Their behavior originates among other reasons, from the presence of weakly or non-coordinating anions, since they have a crucial role in the reactivity enhancement of the complexes, which might be

considered as “naked metal cations” (Strauss 1993; Crossing and Raabe 2004; Vierle et al. 2003, 2004). The anions influence cation stability and the metal accessibility for substrate coordination in intermediate species.

Introduction of weakly coordinating anions into a salt has been done using several methods. Until now, the metathesis of silver salt precursors is the most applied method (Mishra et al. 2013; McCann et al. 1994; Kühn et al. 1999; Pillinger et al. 2001; Rach et al. 2011).

Some of these complexes have been applied as initiators or precursors, in synthesis and catalysis, e.g. in: cyclopropanations (Sakthivel et al. 2006; Syukri et al. 2007; Ajlouni et al. 2019), aziridinations (Mohr et al. 2005; Sakthivel et al. 2005a, b; Li et al. 2008a, b), and polymerizations (Sakthivel et al. 2005a, b; Hijazi et al. 2007a, b, 2008, 2014; Krishnan et al. 2007; Li et al. 2008a, b, 2010; Diebl et al. 2011).

In medicine, several compounds have been activated using the metabolism of metal ions (Mishra et al. 2013). Many metal complexes are used as inhibitors for a variety of bacterial strains (Shelke et al. 2012; Gaballa et al. 2007; Gudasi et al. 2007). Several types of complexes were studied due to their anticancer, antifungal, and antibacterial applications (Ferrari et al. 1999; Canpolat and Kaya 2004; Kostova et al. 2006; Solomon et al. 2007). Bonded metal ions are known as enhancers of the activities of a biologically active species (Ferrari et al. 1999; Kostova et al. 2006).

✉ Ahmed K. Hijazi
akhijazi@just.edu.jo

¹ Department of Chemical Sciences, Faculty of Science and Arts, Jordan University of Science and Technology, P.O. Box 3030, Irbid 22110, Jordan

² Department of Chemistry and Chemical Technology, Tafila Technical University, Tafila, Jordan

³ College of Pharmacy, Al Ain University of Science and Technology, Abu Dhabi, UAE

⁴ Department of Basic Medical Sciences, Faculty of Medicine, Yarmouk University, Irbid, Jordan

Anilines as major contaminants exist in industrial waste water. The oxidation process of anilines to safe substances is very important for many applications, especially industrial ones. The formation of nitrobenzene (White and Emmons 1962), nitrosobenzene (Baumgarten et al. 1965), azoxybenzene (Nezhadali and Akbarpour 2010; Zhao et al. 2011), and azobenzene (Wheeler and Gonzales 1964), using a variety of organic and inorganic oxidants (Emmons 1957; Hijazi et al. 2017; Lima et al. 2018; Meenakshi et al. 2017), is the significant part of this process.

In this work, the synthesis, characterization, as well as the biological and catalytic activities of complexes of general formula $[\text{Fe}^{\text{III}}(\text{NCR})_6][\text{A}]_3$ ($\text{R}=\text{CH}_3, \text{C}_2\text{H}_5$; $\text{A}=[\text{B}(\text{C}_6\text{F}_5)_4]^-$, $[\text{B}(\text{C}_6\text{H}_3)(m\text{-CF}_3)_2]^-$) are reported.

Experimental

All chemicals and solvents have been purchased from Merck Chemical Company and used as is unless stated otherwise. $\text{Ag}[\text{B}(\text{C}_6\text{F}_5)_4]$ and $\text{Ag}[\text{B}(\text{C}_6\text{H}_3)(m\text{-CF}_3)_2]_4$ are prepared according to the literature procedures by Buschmann and Miller (1998) and Hijazi et al. (2008). All complex preparations are done using standard Schlenk techniques under argon atmosphere. A 400 MHz Bruker Avance spectrometer have been used to record the ^{11}B NMR spectra. Chemical shifts are measured in ppm in D_2O with tetramethylsilane (TMS) as an internal standard. Infrared spectra (IR) are recorded with a Bruker Alpha spectrometer in the region of $4000\text{--}400\text{ cm}^{-1}$ using KBr pellets. The spectra are recorded at room temperature with 2 cm^{-1} resolution. A JEOL JES-FA 200 spectrometer has been used to record the EPR spectra. The spectra are measured at 9.25 GHz microwave frequency with 5 mW power, 0.4 mT modulation amplitude, 4 min sweep time, 0.1 s time constant, and 100 kHz modulation frequency. Liquid N_2 is used to cool measurements at 113 K. The g values are determined using Mn^{II} (spin $I=5/2$) embedded in standard magnesium oxide; experimental errors: $\Delta g \pm 0.001$. Thermal studies are performed using a PCT-2A thermo balance analyzer operating at a heating rate of $10\text{ }^\circ\text{C}/\text{min}$ in the range of $30\text{ }^\circ\text{C}$ up to $900\text{ }^\circ\text{C}$ under inert atmosphere. GC-MS data are collected using Varian Saturn 2000 ion trap spectrometer, interfaced with a Varian GC CP-3800 apparatus. Analyses for C, H, and N are determined with a Flash 2000 organic elemental analyzer.

$[\text{Fe}(\text{CH}_3\text{CN})_6][\text{B}(\text{C}_6\text{F}_5)_4]_3$ synthesis

(0.426 mmol, 0.069 g) FeCl_3 is added to a (1.27 mmol, 1.00 g) solution of $\text{Ag}[\text{B}(\text{C}_6\text{F}_5)_4]$ in (15 mL) dry ethyl nitrile. Stirring overnight in dark is made for the mixture. The precipitate is separated from the supernatant, which is concentrated in vacuo at 238 K. The product is obtained

as a brown–orange solid. For $\text{C}_{84}\text{H}_{18}\text{B}_3\text{F}_{60}\text{FeN}_6$ (2339.26): Calcd. C 43.13, H 0.78, N 3.59. Found: C 43.25, H 0.75, N 3.51. Selected IR (KBr, cm^{-1}): $\nu(\text{CN})$, 2311, 2289. ^{11}B -NMR: $\delta = -6.79$. EPR: g value = 2007. Yield 0.81 g (76.4%).

$[\text{Fe}(\text{CH}_3\text{CH}_2\text{CN})_6][\text{B}(\text{C}_6\text{F}_5)_4]_3$ synthesis

(0.426 mmol, 0.069 g) FeCl_3 is added to a (1.27 mmol, 1.00 g) solution of $\text{Ag}[\text{B}(\text{C}_6\text{F}_5)_4]$ in (15 ml) dry propyl nitrile. Stirring overnight in dark is made for the mixture. The precipitate is separated from the supernatant, which is concentrated in vacuo at 238 K. The product is obtained as a brown–orange solid. For $\text{C}_{108}\text{H}_{54}\text{B}_3\text{F}_{72}\text{FeN}_6$ (2891.79): Calcd. C 44.86, H 1.88, N 2.91. Found: C 44.81, H 1.9, N 2.85. Selected IR (KBr, cm^{-1}): $\nu(\text{CN})$, 2319, 2293. ^{11}B -NMR: $\delta = -6.99$. EPR: g value = 2008. Yield 0.79 g (75.9%).

$[\text{Fe}(\text{CH}_3\text{CN})_6][\text{B}(\text{C}_6\text{H}_3)(m\text{-CF}_3)_2]_4$ synthesis

(0.343 mmol 0.055 g) FeCl_3 is added to a (1.03 mmol, 1.00 g) solution of $\text{Ag}[\text{B}(\text{C}_6\text{H}_3)(m\text{-CF}_3)_2]_4$ in (15 ml) dry ethyl nitrile. Stirring overnight in dark is made for the mixture. The precipitate is separated from the supernatant, which is concentrated in vacuo at 238 K. The product is obtained as a brown–orange solid. For $\text{C}_{92}\text{H}_{35}\text{B}_3\text{F}_{60}\text{FeN}_6$ (2452.48): Calcd. C 45.06, H 1.44, N 3.43. Found: C 44.94, H 1.38, N 3.55. Selected IR (KBr, cm^{-1}): $\nu(\text{CN})$, 2318, 2281. ^{11}B -NMR: $\delta = -16.72$. EPR: g value = 2006. Yield 0.72 g (76.9%).

$[\text{Fe}(\text{CH}_3\text{CH}_2\text{CN})_6][\text{B}(\text{C}_6\text{H}_3)(m\text{-CF}_3)_2]_4$ synthesis

(0.343 mmol 0.055 g) FeCl_3 is added to a (1.03 mmol, 1.00 g) solution of $\text{Ag}[\text{B}(\text{C}_6\text{H}_3)(m\text{-CF}_3)_2]_4$ in (15 mL) dry propyl nitrile. Stirring overnight in dark is made for the mixture. The precipitate is separated from the supernatant, which is concentrated in vacuo at 238 K. The product is obtained as a brown–orange solid. For $\text{C}_{114}\text{H}_{66}\text{B}_3\text{F}_{72}\text{FeN}_6$ (2975.95): Calcd. C 46.01, H 2.24, N 2.82. Found: C 45.81, H 2.44, N 2.96. Selected IR (KBr, cm^{-1}): $\nu(\text{CN})$, 2325, 2287. ^{11}B -NMR: $\delta = -6.91$. EPR: g value = 2007. Yield 0.70 g (76.3%).

DFT method

The package of Spartan 14 was used to perform all electronic structure calculations. All geometries were optimized in the gas phase at the B3LYP theory level, which employs the Becke exchange functional parameter B3 (Becke 1993, 1996) and the Lee–Yang–Parr nonlocal correctional functional parameter LYP by Lee et al. (1988), along with the

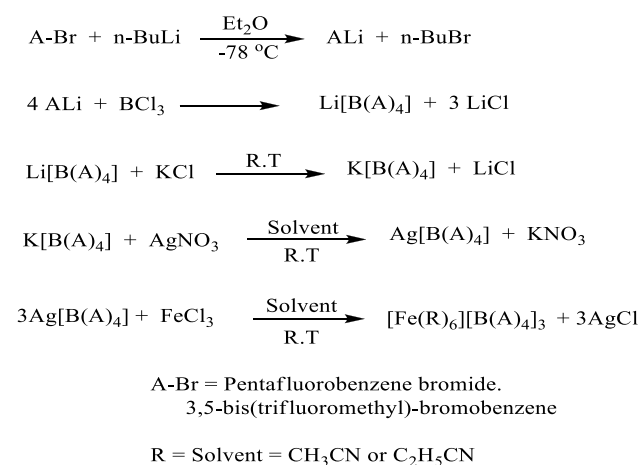
polarized basis set, 6–31G(d), (Petersson et al. 1988, 1991). To ensure the reliability of the selected basis set, the effect of diffuse and polarization functions was inspected by employing the 6–31+G(d,p) basis set at the B3LYP level of theory. Such procedures involving the utilization of a variety of computational methodologies are conducted to essentially assess the validity of selected level of theory and ensure that similar results in terms of structural features and relative energies are produced. Minimal energy structures are indicated by the absence of imaginary frequencies in the vibrational analysis.

Biological properties

The biological properties of all prepared complexes were measured against *Candida albicans*, Gram positive and Gram negative bacteria using micro-broth dilution minimum inhibition concentration, MIC (Hijazi et al. 2017).

Aniline oxidation

To a 30% H₂O₂ solution (10 mmol), 8 mmol of aniline, 7 mL ethyl nitrile or propyl nitrile, and 0.015 mmol of the catalyst are added. The mixture is stirred at ambient temperature overnight. The reaction is continuously followed and GC-MS is used for products identification.



Scheme 1 Synthesis of complexes 1–4

Table 1 Analytical data for complexes 1–4

Complexes	C (%) found (calc.)	H (%) found (calc.)	N (%) found (calc.)	Yields (%)
1	43.25 (43.13)	0.75 (0.78)	3.51 (3.59)	76.4
2	44.81 (44.86)	1.94 (1.88)	2.85 (2.91)	75.9
3	44.94 (45.06)	1.38 (1.44)	3.55 (3.43)	76.9
4	45.81 (46.01)	2.44(2.34)	2.96(2.89)	76.3

Results and discussion

[Fe(CH₃CN)₆][B(C₆F₅)₄]₃ (**1**), [Fe(CH₃CN)₆][B(C₆H₃(m-CF₃)₂)₄]₃ (**2**), [Fe(CH₃CH₂CN)₆][B(C₆F₅)₄]₃ (**3**), and [Fe(CH₃CH₂CN)₆][B(C₆H₃(m-CF₃)₂)₄]₃ (**4**) were synthesized by reacting FeCl₃ with Ag[B(X)₄] in ethyl nitrile and propyl nitrile solvent, Scheme 1. The prepared complexes can be handled in air for short periods of time, since they are only moderately sensitive to air. To keep them catalytically active, the complexes were stored at –40 °C under argon, to prevent decomposition.

Elemental analyses

The elemental analyses and yields of complexes 1–4 are listed in Table 1. Based on the proposed molecular formula, an agreement between the calculated elemental contents and the obtained ones are obvious, indicating the correctness of the assumed composition of the prepared complexes.

Infrared spectroscopy

Two sharp bands of medium intensity are observed for all complexes at 2311 and 2289 cm^{–1}, at 2319 and 2293 cm^{–1}, at 2318 and 2281 cm^{–1}, and at 2325 and 2287 cm^{–1}, respectively. Fundamental stretching (ν_2) and ($\nu_3 + \nu_4$) modes of CN are responsible for these bands. Presence of the ligands (ethyl nitrile and propyl nitrile) in the inner sphere of complexes is confirmed by these results, see Table 2, Fig. 1.

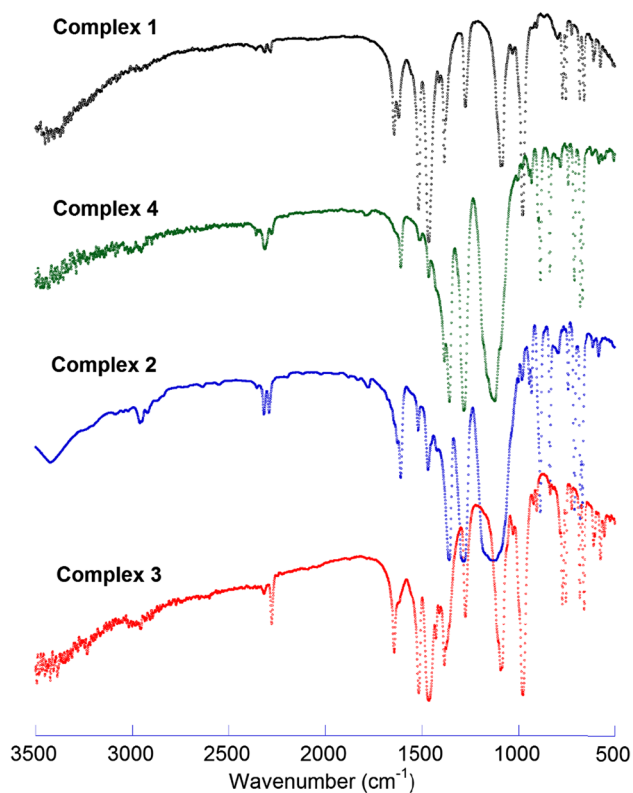
Due to the σ -donation of electron density from the lone pair on nitrogen, the observed vibrations have higher energies compared to the corresponding vibrations of free acetonitrile (Buschmann and Miller 1998; Pratikha et al. 2013), and propionitrile (Hijazi et al. 2016). The respective orbitals have some *anti*-bonding character (Pratikha et al. 2013; Higa et al. 2010; Shriver et al. 1965).

Two peaks at 3045 and 891 cm^{–1}, and 3040 and 895 cm^{–1} are observed for complex 2 and complex 4, respectively. These peaks are attributed to the aromatic C–H of the counter anion. These peaks are not observed for complexes 1 and 3.

The aromatic C=C bonds of all complexes are identified with the peaks at 1620 and 1450 cm^{–1}, 1602 and 1471 cm^{–1},

Table 2 FT-IR spectral data for complexes 1–4 (cm^{-1})

Complexes	$\nu(\text{CN})$		$\nu[\text{Ar}-(\text{C}-\text{H})]$		$\nu[\text{Ar}-(\text{C}=\text{C})]$		$\nu[\text{Ar}-(\text{C}-\text{F})]$		
1	2311	2289	–	–	1620	1450	1381	1273	1091
2	2319	2293	3045	891	1602	1471	1358	1283	1121
3	2318	2281	–	–	1643	1445	1382	1276	1088
4	2325	2287	3040	895	1601	1475	1357	1280	1125

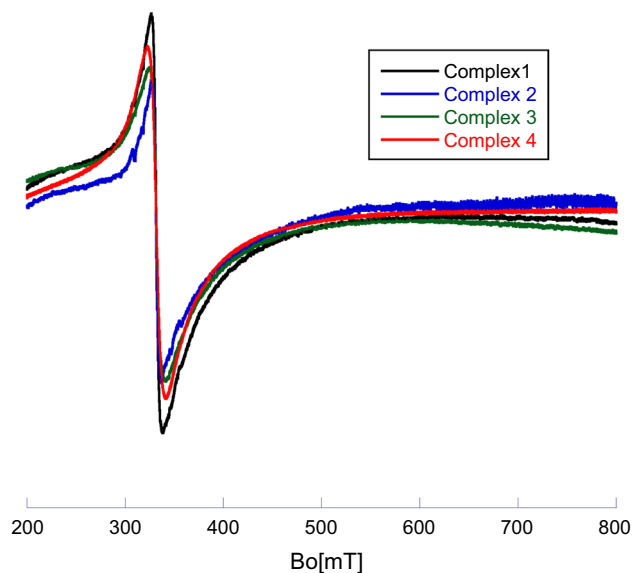
**Fig. 1** FT-IR spectrum of complexes 1–4**Table 3** The EPR data for complexes 1–4

Metal complex	<i>g</i> value
1	2007
2	2008
3	2006
4	2007

1643 and 1445 cm^{-1} , and at 1601 and 1475 cm^{-1} for complexes 1, 2, 3, and 4, respectively, Table 2, Fig. 1.

Electron paramagnetic resonance (EPR)

The spectra of $[\text{Fe}(\text{C}_2\text{H}_5\text{CN})_6]^{3+}$ and $[\text{Fe}(\text{CH}_3\text{CN})_6]^{3+}$ with varying counter ions, ($T_{\text{rec}} = -140^\circ\text{C}$) have symmetric lines ($B_{\text{pp}} = 9$ mT) at $g = 2.006\text{--}2.008$, Table 3, in frozen solution. This signal, Fig. 2, is consistent with iron(III) high-spin

**Fig. 2** EPR spectrum of complexes 1–4, $T_{\text{rec}} = -140^\circ\text{C}$

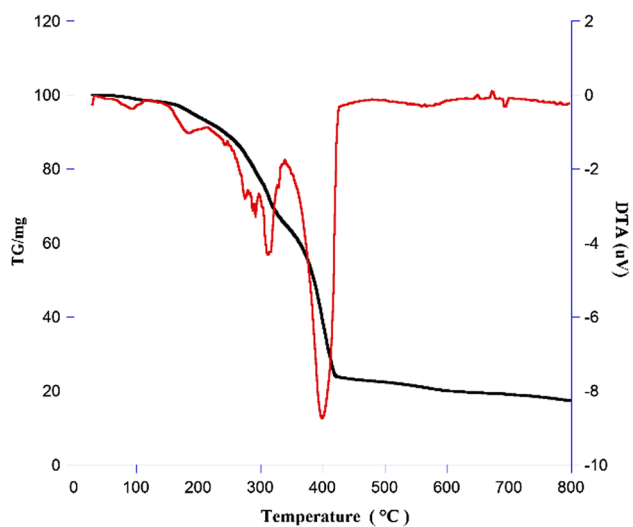
complexes ($S = 5/2$). A shift in the g value from one of the free electrons is observed, as expected.

Thermal gravimetric analysis

Thermo gravimetric (TG) and differential thermal analysis (DTA) were done within a temperature interval, ranging from 30 $^\circ\text{C}$ to 800 $^\circ\text{C}$ under N_2 flow. Table 4 shows the data of thermal analysis of all complexes. The TGA-DTG curve of complex 1, shows the first onset is at 51 $^\circ\text{C}$, with 7.11 wt% mass loss. The loss of four ethyl nitrile ligands is associated to this step (calc. 7.03 wt%). The second step onset at 106 $^\circ\text{C}$, with a mass loss of 4.94 wt%, shows the loss of two acetonitrile ligands (calc. 3.52 wt%). A similar behavior is also observed for complex 2, the first decomposition onset being observed at 55 $^\circ\text{C}$, with a loss of 4.35 wt%. This corresponds to the loss of three ethyl nitrile ligands (calc. 4.26 wt%). The second onset at 165 $^\circ\text{C}$ is with a mass loss of 23.67 wt%. This mass loss corresponds to the loss of three of the ethyl nitrile ligands and to anion fragmentation $[\text{B}\{\text{C}_6\text{H}_3(\text{m}-\text{CF}_3)_2\}_4]$. These ligands contribute 4.26 wt% of the total mass complex 2. Complex 3 shows its 1st decomposition step at 68 $^\circ\text{C}$ with 9.00 wt% loss corresponding to four propionitrile ligands (calc. 8.44 wt%). The second step

Table 4 TGA data for complexes 1–4

Complex	Stage	DTA/C	Mass loss %	Total mass loss %
1	1	51	7.11	83.65
	2	106	4.94	
	3	194	28.42	
	4	315	35.00	
	5	446	8.18	
2	1	55	4.35	81.63
	2	165	23.67	
	3	368	50.07	
	4	502	3.54	
3	1	81	9.00	86.45
	2	239	67.74	
	3	362	5.38	
	4	435	4.78	
4	1	90	2.07	80.90
	2	180	5.53	
	3	309	29.67	
	4	401	38.1	
	5	565	5.53	

**Fig. 3** TGA/TDA spectra of complex 4

is at 239 °C with loss of 64.2 wt%. This step shows the loss of two propyl nitrile ligands (calc. 3.43 wt%) and for anion fragmentation. The first and second decomposition steps of complex 4 have been detected at 90 °C and 180 °C with a loss of 2.07 wt% and 5.53 wt%, respectively, as shown in Fig. 3. These steps correspond to the loss of one propionitrile (calc. 1.71 wt%) and three propionitrile ligands (calc. 5.14 wt%), respectively. The third step at 309 °C is associated with a 29.67 wt% loss. It accounts for the loss of two propionitrile ligands and for fragmentation of the counter anion. Complex 4 has the highest stability and loses

the lowest mass in the examined temperature interval, with a total 80.90% weight loss, while complex 1 has the lowest stability of all complexes. Complex 3 loses the highest relative mass, with a total weight loss of 86.45 wt%. The residual mass in all complexes indicates the presence of FeF₃, (for complex 1 5.09 wt% (calc. 4.8%), complex 2 4.0 wt% (calc. 3.8%), complex 3 4.8 wt% (calc. 4.6%), and complex 4 3.9 wt% (calc. 3.6%) after decomposition. The DTA correspondingly shows a strong endothermic signal through all decomposition steps.

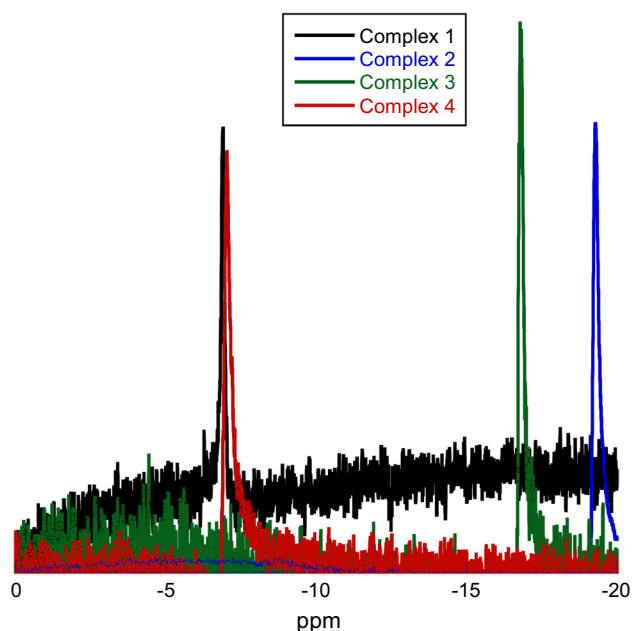
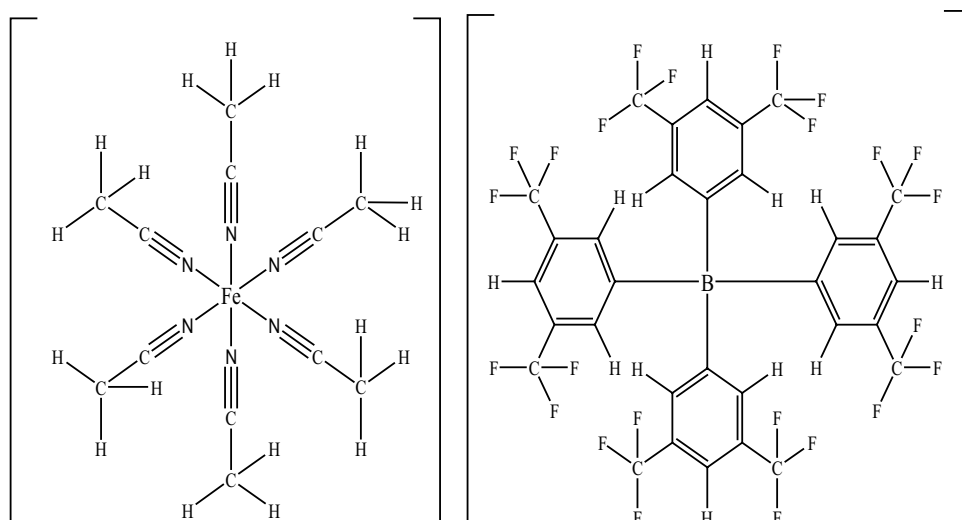
Figure 4 shows the proposed or the expected structure of complex 2, which applies to all prepared complexes.

¹¹B-NMR

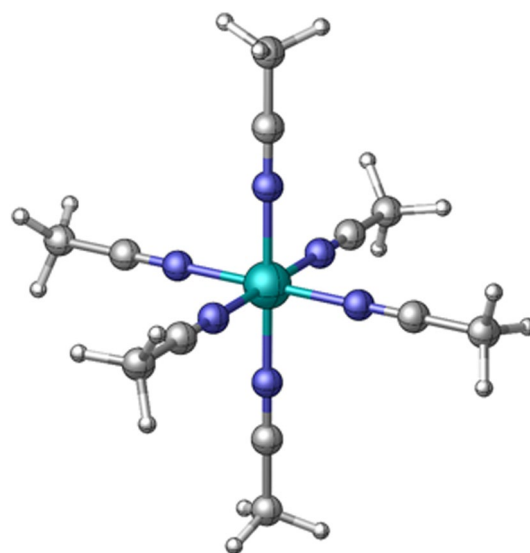
The ¹¹B-NMR spectra were recorded in deuterium oxide (D₂O), in the range of (–25 to 15) ppm. Singlet peaks at $\delta = -16.72$ ppm and $\delta = -6.79$ ppm are assigned to the B atom of the [B(C₆F₅)₄] counter anion of complexes 3 and 1, respectively. A singlet peak at $\delta = -6.99$ ppm and $\delta = -6.91$ ppm are assigned to the boron atom of the [B{C₆H₃(m-CF₃)₂]₄] counter anion of complex 2 and complex 4, respectively, Fig. 5.

DFT calculations

The optimized structures of complexes 3 and 4 at the B3LYP/6-31G(d) level of theory are shown in Figs. 6, 7. Results confirm that both complexes exhibit six coordination number (*O_h*) with the Fe³⁺. Due to high symmetry, all bonds and angles of the same type have the same or very close structural parameters. Complex 3 has an identical C–N bond distance for the six groups at 1.157 Å. The average Fe–N bond distance is shown to be 1.940 Å with average N–Fe–N angles of 90.00° and 179.95°. Considering the similarity in the coordination environment around the iron ion in these complexes, complex 4 exhibits similar structural features. For complex 4, the results show that the average Fe–N bond distance is 1.938 Å and the average N–Fe–N angles are 90.00° and 179.78°. The C–N bond is at a calculated value of 1.158 Å. Selected bond lengths (Å) and angles (°) of complexes 1 and 2 ground state optimized geometries are listed in Table 5. As can be seen from the table, the structural features emanating from both the B3LYP/6-31G(d) and B3LLYP/6-31+G(d,p) levels of theory are very comparable resulting in no more than 0.002 Å and 0.24° discrepancy in bond lengths and angles, respectively. Vibrational analysis for complex 3 reveals a strong absorption band compromising the wavenumbers 2299 and 2315 cm^{–1} and attributed to $\nu(\text{CN})$ (exp. 2281 and 2318 cm^{–1}). This characteristic band appears at 2276 and 2301 cm^{–1} in the calculated IR spectrum of complex 4 (exp. 2287 and 2325 cm^{–1}). Furthermore, molecular

Fig. 4 Proposed structure of complex **2****Fig. 5** ¹¹B-NMR of complexes **1–4**

electrostatic potential (MEP) maps were constructed for both complexes. These surfaces illustrate the charge distributions of molecules by mapping the calculated value of the electrostatic potential onto an electron density surface. Such maps bear useful information on the shape, overall size of molecules, and how they interact with other molecules. Figure 8 depicts the electrostatic potential maps for complexes **3** (left) and **4** (right), along with a color scale indicating the positive and negative electrostatic potentials. By convention, red-colored regions correspond to minimum negative electrostatic potential, while colors toward blue represent maximum positive potential. In

**Fig. 6** The optimized geometry for complex **3** at the B3LYP/6-31G(d) level of theory

consistent with the cationic nature of studied complexes, all electrostatic potential values for complexes **3** and **4** are found on the positive side of potential distribution ranging from 785–930 and 645–894 kJ/mol, respectively. While regions with most electropositive potential are located around the central metal ion and the carbon atom of the CN group (thus more prone to nucleophilic attack), terminal methyl groups bare relatively the most electronegative potentials.

The harmony between the experimental structure parameters and the calculated structure parameters confirms the suitability of the experimental and calculation structures (Erkan and Karakas 2019).

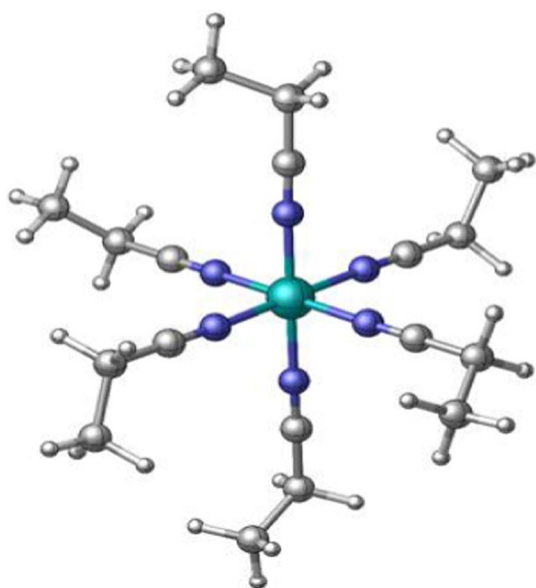
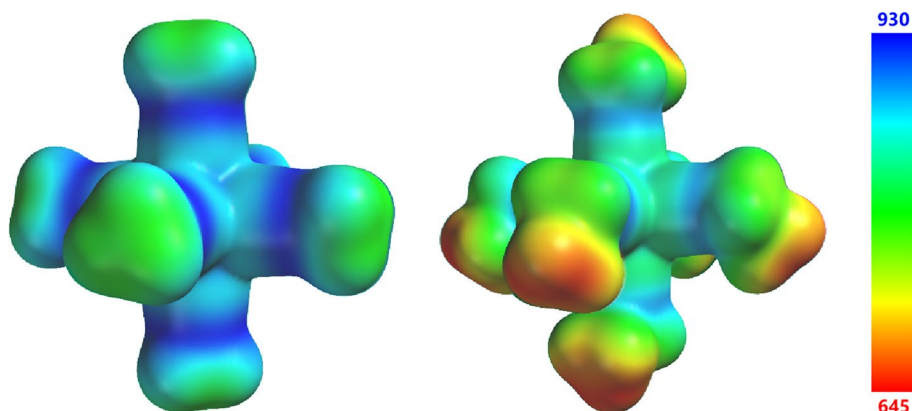


Fig. 7 The optimized geometry for complex **4** at the B3LYP/6-31G(d) level of theory

Table 5 Selected bond lengths (Å) and angles (°) of complexes **3** and **4** at the B3LYP/6-31G(d) and B3LYP/6-31+G(d, p) levels of theory

Bond/angle	Complex 3		Complex 4	
	6-31G(d)	6-31+G(d,p)	6-31G(d)	6-31+G(d,p)
Fe–N	1.940	1.942	1.938	1.940
C–N	1.157	1.158	1.158	1.158
NC–C	1.452	1.452	1.460	1.460
H ₂ C–CH ₃	NA	NA	1.548	1.548
N–Fe–N	179.95	179.96	179.78	179.79
N–Fe–N	90.00	90.00	90.00	90.00
C–C–C	NA	NA	113.16	113.40

Fig. 8 Electrostatic potential maps for complex **3** (left) and **4** (right)



Biological properties

Minimum inhibitory concentration determination

Minimum inhibitory concentration (MIC, $\mu\text{g}/\text{cm}^3$) of all complexes are listed in Table 6. The complexes have different MIC degrees on the bacterial strain growth and *Candida albicans* tested. The results show that complexes **1** and **3** exhibit a broad and promising spectrum of antibacterial and antifungal profiles against the tested organisms. Complex **2** shows moderate antibacterial activity against *Klebsiella pneumonia* (Gram negative) and low antibacterial activity against *Bacillus cereus* and *Staphylococcus aureus* (Gram positive). Complex **4** shows moderate antibacterial activity against *Streptococcus pyogenes* (Gram positive) and low antibacterial activity against *Escherichia coli*, *Proteus mirabilis*, *Staphylococcus aureus*, and *Pseudomonas aeruginosa*, while it was not effective against *Klebsiella pneumonia*, *Salmonella enteritidis*, and *Bacillus cereus*. The activity against *C. albicans* (fungal) has been detected for both complexes. All complexes **1–4** have similar geometries, but the results show that the nature of ligands affects their activity. Hydrogen bonding between the ligands is facilitated and chelating character occurs. Types of anions and the lipophilic nature might be responsible for some interactions with selected microorganisms, which will increase the complexes' penetration of the lipid membrane of the cell wall of the microorganism, increasing the complex activity and restricting the possible growth of the affected organism (Singh et al. 2012). The activity against Gram (+) species can be explained by taking into consideration the effect on lipopolysaccharides (LPS) (Al Momani et al. 2013). LPS are crucial to determine the virulence of the outer membrane barrier function and Gram negative pathogens. The complexes described here can penetrate the cell membrane by coordination of the metal through nitrogen atoms to LPS, leading to the damage of the outer cell membrane and consequently inhibiting the bacterial growth (Priya et al. 2009).

Table 6 MIC ($\mu\text{g/mL}$) of all complexes against clinical isolates of some bacterial spp., and *Candida albicans*

Tested compounds	Gram (–) bacteria				Gram (+) bacteria				Antifungal
	Ec	Kp	Pm	Pa	Se	Sa	Sp	Bc	Ca
1	256	32	32	256	265	16	N	8	16
2	N	64	N	N	N	256	N	256	128
3	256	16	256	128	256	16	N	64	32
4	256	N	256	512	N	256	64	N	32
DMSO (–ve control)	N	N	N	N	N	N	N	N	N
Oxytetracycline (+ve control)	4	2	8	2	8	8	8	8	–
Fluconazole (+ve control)	–	–	–	–	–	–	–	–	4

Ec, *Escherichia coli*; *Kp*, *Klebsiella pneumoniae*; *Pm*, *Proteus mirabilis*; *Pa*, *Pseudomonas aeruginosa*; *Se*, *Salmonella enteritidis*; *Sa*, *Staphylococcus aureus*; *Ca*, *Candida albicans*; *Bc* *Bacillus cereus*; *Sp*, *Streptococcus pyogenes*

Fluconazole: antifungal positive control for *Candida albicans*

Oxidation of aniline

Prepared complexes were used as catalysts for aniline oxidation and its derivatives using 30% H_2O_2 with 1:10 catalyst/aniline weight ratio and ethyl nitrile or propyl nitrile as solvents at room temperature, for 24 h. GC-MS have been used to monitor the reaction. During the reaction, azobenzene is identified as a product (Scheme 2).

Complex **2** leads to higher yields (24%) than complex **1** (9%), and when acetonitrile is replaced by propionitrile as a ligand, the yields become much higher as observed for complex **3** (43%) and complex **4**, which displays the highest yields (61%). This could be attributed to the solubility factor, which leads to a better iron exposition. Since complex **4** produces the highest oxidation yield, it was additionally applied as a catalyst for the oxidation of some

aniline derivatives (see Table 7). A very good yield (62%) was reported for 2-nitro-4-(trifluoromethyl) aniline, other derivatives range from low to moderate yields. The applied derivatives of aniline display either electron withdrawing or electron donating groups. The derivatives having electron donating groups are oxidized only in low yields, ranging from 14 to 17%, while ones having electron withdrawing groups display higher yields when oxidation, namely 23–62%. It has to be noted that with increasing strength of the electron withdrawing effect increases the %yield. In all complexes, azobenzene is the only product with 100% selectivity according to the GC-MS data.

The same amount of H_2O_2 was used to examine the oxidation of aniline absence of the metal complexes; this led to very low yields only (ca. 1–2%). When the reaction was done using only the catalyst in the absence of H_2O_2 , no product was obtained.

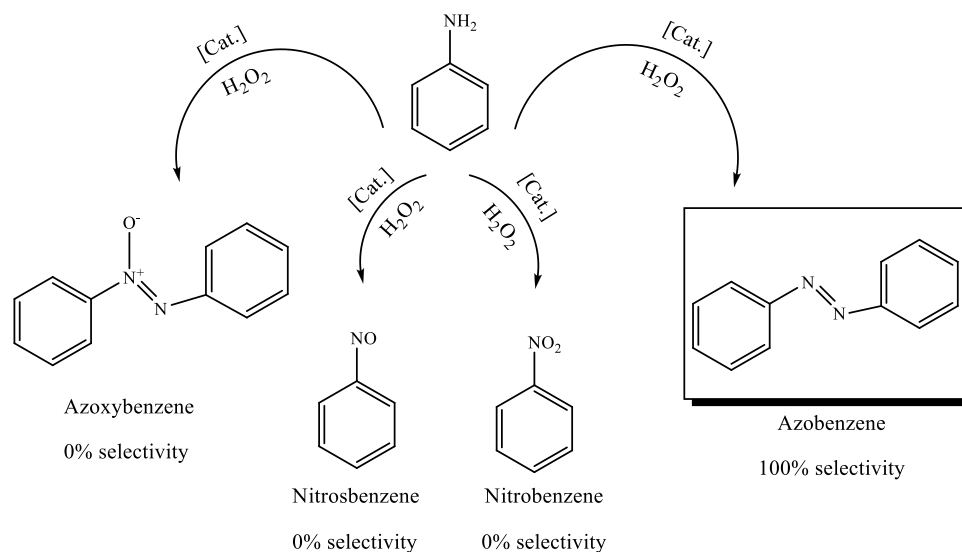
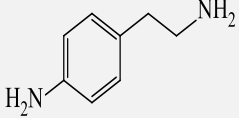
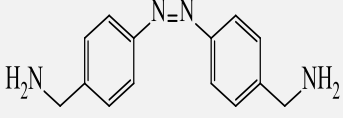
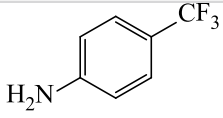
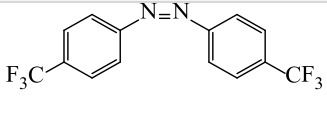
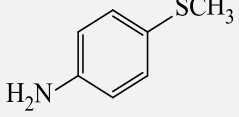
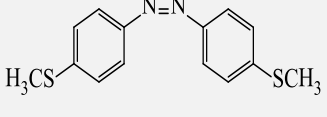
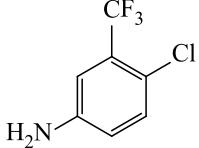
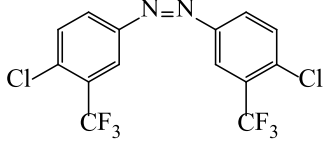
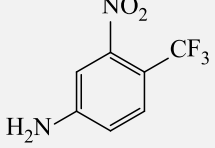
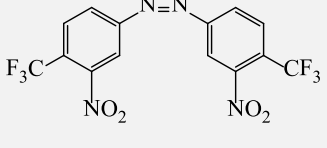
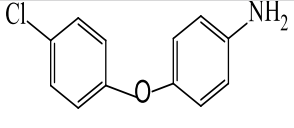
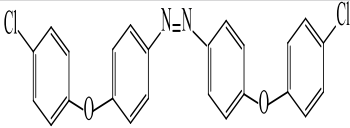
Scheme 2 Oxidation of aniline to azobenzene

Table 7 Oxidation of various aniline derivatives with complex **1** after 24 h

Entry	Reactant	Product	%Yield ^a	Selectivity(%) ^b
1			14%	100
2			23%	100
3			17%	100
4			35%	100
5			62%	100
6			29%	100

$T=298\text{ K}$, $t=24\text{ h}$, H_2O_2 : aniline: cat. (10: 8: 0.015 mmol), solvent: CH_3CN

^{a, b}Based on GC-MS data

Conclusion

Fe(III) complexes, $[\text{Fe}(\text{CH}_3\text{CN})_6][\text{X}]_3$ and $[\text{Fe}(\text{CH}_3\text{CH}_2\text{CN})_6][\text{X}]_3$ (where X: counter anion = $\text{B}\{\text{C}_6\text{H}_3(\text{m}-\text{CF}_3)_2\}_4\text{)}^-$ and $\text{B}(\text{C}_6\text{F}_5)_4^-$) have been prepared with very good yields and characterized. DFT calculations show that the structures, proposed on spectroscopic data agree with the calculated ones. All complexes have been used as catalysts for aniline oxidation and some derivatives. Complex **4** showed the highest yield (61%) when aniline was oxidized to produce azobenzene. A maximum yield of 62% could be obtained for the most

electron deficient aniline using complex **4**. Azobenzene have been determined as the only product depending on GC-MS data with 100% selectivity. Antimicrobial effects have been studied for all synthesized complexes. Complex **1** showed promising antimicrobial activities against *Sa* and *Bc* (Gram-positive bacteria), *Kp* and *Pm* (Gram-negative bacteria), and *Ca* (fungal). Complex **3** exhibited promising activities against *Kp* (Gram-negative bacteria), *Sa* (Gram-positive bacteria), and *Ca* (fungal).

Acknowledgements The Deanship of Research, Jordan University of Science and Technology are acknowledged for the financial support (Grant no. 360/2015).

Compliance with ethical standards

Conflict of interest The author declares that they have no competing interests.

References

- Ajlouni AM, Hijazi AK, Taha ZA, Al Momani W, Okour A, Kühn FE (2019) Synthesis, characterization and biological and catalytic activities of propionitril: ligated transition metal complexes with $[B(C_6F_5)_4]$ as counter anion. *Catal Lett*. <https://doi.org/10.1007/s10562-019-02804-9>
- Al Momani WM, Taha ZA, Ajlouni AM, Abu Shaqra QM, Al Zoubi M (2013) A study of in vitro antibacterial activity of lanthanides complexes with a tetradentate Schiff base ligand. *Asian Pac J Trop Biomed* 3:367–370. [https://doi.org/10.1016/S2221-1691\(13\)60078-7](https://doi.org/10.1016/S2221-1691(13)60078-7)
- Angerman NS, Jordan RB (1969) Line broadening of the proton magnetic resonance of nonaqueous solvents by vanadyl ion. *Inorg Chem* 8:65–69. <https://doi.org/10.1021/ic50071a016>
- Baumgarten HE, Staklis A, Miller EM (1965) Reactions of amines. XIII. The oxidation of N-Acyl-N-arylhydroxylamines with lead tetraacetate 1,2. *J Org Chem* 30:1203–1206. <https://doi.org/10.1021/jo01015a058>
- Becke AD (1993) Density-functional thermochemistry. III. The role of exact exchange. *J Chem Phys* 98:5648–5652. <https://doi.org/10.1063/1.464913>
- Becke AD (1996) Density-functional thermochemistry. IV. A new dynamical correlation functional and implications for exact-exchange mixing. *J Chem Phys* 104:1040–1046. <https://doi.org/10.1063/1.470829>
- Buschmann WE, Miller JS (1998) Sources of naked divalent first-row metal ions: synthesis and characterization of $[M^{II}(NCMe)_6]^{2+}$ (M=V, Cr, Mn, Fe Co, Ni) Salts of Tetrakis[3,5-bis(trifluoromethyl)phenyl]borate. *Chem Eur J* 4:1731–1737. [https://doi.org/10.1002/\(SICI\)1521-3765\(19980904\)4:9%3c1731:AID-CHEM1731%3e3.0.CO;2-U](https://doi.org/10.1002/(SICI)1521-3765(19980904)4:9%3c1731:AID-CHEM1731%3e3.0.CO;2-U)
- Buschmann WE, Miller JS (2002) Useful reagents and ligands. *Inorg Synth* 33:83–89. <https://doi.org/10.1002/0471224502>
- Canpolat E, Kaya M (2004) Studies on mononuclear chelates derived from substituted Schiff-base ligands (part 2): synthesis and characterization of a new 5-bromosalicyliden- p-aminoacetophenoneoxime and its complexes with Co(II), Ni(II), Cu(II) and Zn(II). *J Coord Chem* 57:1217–1223. <https://doi.org/10.1080/00958970412331285913>
- Cotton FA, Kühn FE (1996) Dimolybdenum compounds with cross-wise-bridging acetonitrile molecules. *J Am Chem Soc* 118:5826–5827. <https://doi.org/10.1021/ja954262q>
- Diebl BE, Yeong HY, Cokoja M, Herdtweck E, Voit B, Kühn FE (2011) Synthesis and catalytic application of monometallic molybdenum(IV) nitrile complexes. *Tett Lett* 52:955–959. <https://doi.org/10.1016/j.tetlet.2010.12.059>
- Emmons WD (1957) The oxidation of amines with peracetic acid. *J Am Chem Soc* 79:5528–5530. <https://doi.org/10.1021/ja01577a053>
- Erkan S, Karakas D (2019) DFT investigation and molecular docking studies on dinuclear metal carbonyls containing pyridyl ligands with alkyne unit. *Chem Pap* 73:2387–2398. <https://doi.org/10.1007/s11696-019-00784-z>
- Ferrari MB, Capacchi S, Pelosi G, Reffo G, Tarasconi P, Albertini R, Pinelli S, Lunghi P (1999) Synthesis, structural characterization and biological activity of helicin thiosemicarbazone monohydrate and a copper(II) complex of salicylaldehyde thiosemicarbazone. *Inorg Chim Acta* 286:134–141. [https://doi.org/10.1016/S0020-1693\(98\)00383-1](https://doi.org/10.1016/S0020-1693(98)00383-1)
- Gaballa AS, Asker MS, Barakat AS, Teleb SM (2007) Synthesis, characterization and biological activity of some platinum(II) complexes with Schiff bases derived from salicylaldehyde, 2-furaldehyde and phenylenediamine. *Spectro Chim Acta A* 67:114–121. <https://doi.org/10.1016/j.saa.2006.06.031>
- Gudasi KB, Havanur VC, Patil SA, Patil BR (2007) Antimicrobial study of newly synthesized lanthanide(III) complexes of 2-[2-hydroxy-3-methoxyphenyl]-3-[2-hydroxy-3-methoxybenzylamino]-1,2-dihydroquinazolin-4(3H)-one. *Metal Based Drugs*. <https://doi.org/10.1155/2007/37348> (7 pages)
- Hathaway BJ, Holah DG (1964) Transition-metal halide–methyl cyanide complexes. Part I. Manganese, cobalt, and nickel. *J Chem Soc*. <https://doi.org/10.1039/JR9640002400>
- Henriques RT, Herdtweck E, Kühn FE, Lopes AD, Mink J, Romão CC (1998) Synthesis, characterization, and reactions of tetrakis(nitrile)chromium(II) tetrafluoroborate complexes. *J Chem Soc, Dalton Trans*. <https://doi.org/10.1039/A708988K>
- Higa T, Fukui M, Fukui K, Naganuma Y, Kajita Y (2010) Simplified bicyclic cage-type molecule as a C 3 -symmetric host: X-ray and FTIR characterization of encapsulation of a nitrile molecule. *J Incl Phen Macro Chem* 66:171–177. <https://doi.org/10.1007/s10847-009-9681-z>
- Hijazi AK, Yeong HY, Zhang Y, Herdtweck E, Nuyken O, Kühn FE (2007a) Isobutene Polymerization Using $[Cu^{II}(NCMe)_6]^{2+}$ with Non-Coordinating Anions as Catalysts. *Macromol Rapid Commun* 28:670–675. <https://doi.org/10.1002/marc.200600139>
- Hijazi AK, Krishnan NR, Jain KR, Herdtweck E, Nuyken O, Walter HM, Hanefeld P, Voit B, Kühn FE (2007b) Molybdenum(III) compounds as catalysts for 2-methylpropene polymerization. *Angew Chem Int Ed* 46:7290–7293. <https://doi.org/10.1002/anie.200700748>
- Hijazi AK, Al Hmaideen A, Syukri S, Krishnan NR, Herdtweck E, Voit B, Kühn FE (2008) Synthesis and characterization of acetonitrile-ligated transition-metal complexes with tetrakis(pentafluorophenyl)borate as counteranions. *Eur J Inorg Chem*. <https://doi.org/10.1002/ejic.200800201>
- Hijazi AK, Taha ZA, Ajlouni A, Radhakrishnan N, Voit B, Kühn FE (2014) Improved synthesis, characterization and catalytic application of $[H(OEt_2)_2][B\{C_6H_3(m-CF_3)_2\}_4]$. *J Organomet Chem* 763–764:65–68. <https://doi.org/10.1016/j.jorganchem.2014.04.023>
- Hijazi AK, Taha ZA, Ajlouni AM, Al-Momani WM, Ababneh TS, Alshare HM, Kühn FE (2016) Synthesis, catalytic and biological activities and computational study of Fe(III) solvent-ligated complexes having B(Ph)₄ as counter anion. *Appl Organometal Chem*. <https://doi.org/10.1002/aoc.3601>
- Hijazi AK, Taha ZA, Ajlouni AM, Al-Momani WM, Idris IM, Abu Hamra O (2017) Synthesis and biological activities of lanthanide (III) nitrate complexes with N-(2-hydroxynaphthalen-1-yl) methylene) nicotinohydrazide schiff base. *Med Chem* 13:77–84. <https://doi.org/10.2174/1573406412666160225155908>
- Johnson PR, Pratt JM, Tilley RI (1978) Experimental determination of the standard reduction potential of the gold(I) ion. *J Chem Soc, Chem Commun*. <https://doi.org/10.1039/C39780000606>
- Kostova I, Momekov G, Tzanova T, Karaivanova M (2006) Synthesis, characterization, and cytotoxic activity of new lanthanum(III) complexes of bis-coumarins. *Bioinorg Chem Appl*. <https://doi.org/10.1155/BCA/2006/25651> (9 pages)
- Krishnan NR, Hijazi AK, Komber H, Voit B, Zschoche S, Kühn FE, Nuyken O, Walter M, Hanefeld P (2007) Synthesis of highly reactive polyisobutylenes using solvent-ligated manganese(II) complexes as catalysts. *J Polym Sci, Part A: Polym Chem* 45:5636–5648. <https://doi.org/10.1002/pola.22312>

- Krossing I, Raabe I (2004) Noncoordinating anions—fact or fiction? A survey of likely candidates. *Angew Chem Int Ed* 43:2066–2090. <https://doi.org/10.1002/anie.200300620>
- Kühn FE, Ismeier JR, Schön D, Xue WM, Zhang G, Nuyken O (1999) Solvent stabilized transition metal cations as initiators for cyclopentadiene polymerization. *Macromol Rapid Commun* 20:555–559. [https://doi.org/10.1002/\(SICI\)1521-3927\(19991001\)20:10%3c555:AID-MARC555%3e3.0.CO;2-V](https://doi.org/10.1002/(SICI)1521-3927(19991001)20:10%3c555:AID-MARC555%3e3.0.CO;2-V)
- Lee C, Yang W, Parr RG (1988) Development of the colle-salveti correlation-energy formula into a functional of the electron density. *Phys Rev B* 37:785–789. <https://doi.org/10.1103/PhysRevB.37.785>
- Li Y, Diebl B, Raith A, Kühn FE (2008a) Syntheses of acetonitrile ligated copper complexes with perfluoroalkoxy aluminate as counter anion and their catalytic application for olefin aziridination. *Tet Lett* 49:5954–5956. <https://doi.org/10.1016/j.tetlet.2008.07.162>
- Li Y, Voon LT, Yeong HY, Hijazi AK, Krishnan NR, Köhler K, Voit B, Nuyken O, Kühn FE (2008b) Solvent-ligated copper(II) complexes for the homopolymerization of 2-methylpropene. *Chem Eur J* 14:7997–8003. <https://doi.org/10.1002/chem.200701928>
- Li Y, Yeong HY, Herdtweck E, Voit B, Kühn FE (2010) Synthesis, characterization and application of nitrile-ligated zinc(II) complexes incorporating (Fluoroalkoxy)aluminates. *Eur J Inorg Chem*. <https://doi.org/10.1002/ejic.201000724>
- Liang HC, Kim E, Incarvito CD, Rheingold AL, Karlin KD (2002) A bis-acetonitrile two-coordinate copper(I) complex: synthesis and characterization of highly soluble $B(C_6F_5)_4^-$ Salts of $[Cu(MeCN)_2]^+$ and $[Cu(MeCN)_4]^+$. *Inorg Chem* 41:2209–2212. <https://doi.org/10.1021/ic010816g>
- Lima ALD, Batalha DG, Fajardo HV, Rodrigues JL, Periera MG, Silva AG (2018) Room temperature selective conversion of aniline to azoxybenzene over an amorphous niobium oxyhydroxide supported on δ -FeOOH. *Catal Today*. <https://doi.org/10.1016/j.catto.2018.10.035>
- McCann M, Coda EMG, Maddock K (1994) $[Mo_2(MeCN)_8][BF_4]_4$ supported on silica: an efficient heterogeneous catalyst for the ring-opening metathesis polymerization of norbornene. *J Chem Soc, Dalton Trans*. <https://doi.org/10.1039/DT9940001489>
- Meenakshi R, Shakeela K, Kutti Rani S, Ranga Rao G (2017) Oxidation of aniline to nitrobenzene catalysed by 1-butyl-3-methyl imidazolium phosphotungstate hybrid material using m-chloroperbenzoic acid as an oxidant. *Catal Lett*. <https://doi.org/10.1007/s10562-017-2214-2>
- Mishra N, Poonia K, Kumar D (2013) A Practical, fast, and high-yielding aziridination procedure using simple Cu(II) complexes containing N-donor pyridine-based ligands. *Int J Adv Res Technol* 2:52–66. <https://doi.org/10.1021/jo050485f>
- Mohr F, Binfield SA, Fettinger JC, Vedernikov AN (2005) Selective oxidation of primary substituted aromatic amines to azoxy products using lacunary catalyses. *J Org Chem* 70:4833–4839. <https://doi.org/10.1016/j.joclet.2009.07.017>
- Nezhadali A, Akbarpour M (2010) Near infrared spectroscopic observation of the linear and cyclic isomers of the hydrogen cyanide trimer. *Chin Chem Lett* 21:43–46. <https://doi.org/10.1063/1.454052>
- Petersson GA, Bennett A, Tensfeldt TG, Al-Laham MA, Shirley WA, Mantzaris JA (1988) A complete basis set model chemistry. III. The complete basis set-quadratic configuration interaction family of methods *J Chem Phys* 89:2193–2218. <https://doi.org/10.1063/1.460448>
- Petersson GA, Tensfeldt TG, Montgomery JA Jr (1991) A complete basis set model chemistry. III. The complete basis set-quadratic configuration interaction family of methods. *J Chem Phys* 94:6091–6101. <https://doi.org/10.1063/1.460448>
- Pillinger M, Gonçalves IS, Ferreira P, Rocha J, Schäfer M, Schön D, Nuyken O, Kühn FE (2001) Multiply bonded dimolybdenum cation immobilized in mesoporous silica: XAFS analysis and catalytic activity in cyclopentadiene polymerization. *Macromol Rapid Commun* 22:1302–1305. [https://doi.org/10.1002/1521-3927\(20011101\)22:16%3c1302:AID-MARC1302%3e3.0.CO;2-5](https://doi.org/10.1002/1521-3927(20011101)22:16%3c1302:AID-MARC1302%3e3.0.CO;2-5)
- Pratikha RS, Syukri S, Admi A (2013) Synthesis and characterization of acetonitrile ligated Cu(II)-complex and its Catalytic application for transesterification of frying oil in heterogeneous phase. *Indon J Chem* 13:72–76. <https://doi.org/10.22146/ijc.21329>
- Priya NP, Arunachalam S, Manimaran A, Muthupriya D, Jaya Balakrishnan C (2009) Mononuclear Ru(III) Schiff base complexes: Synthesis, spectral, redox, catalytic and biological activity studies. *Spectrochim Acta A* 72:670–676. <https://doi.org/10.1016/j.saa.2008.10.028>
- Rach SF, Kühn FE (2009) Nitrile ligated transition metal complexes with weakly coordinating counteranions and their catalytic applications. *Chem Rev* 109:2061–2080. <https://doi.org/10.1021/cr800270h>
- Rach SF, Herdtweck E, Kühn FE (2011) A straightforward synthesis of cationic nitrile ligated transition metal complexes with the $[B(C_6F_5)_4]^-$ anion. *J Organomet Chem* 696:1817–1823. <https://doi.org/10.1016/j.jorganchem.2011.02.008>
- Rapaport I, Helm L, Merbach AE, Bernhard P, Ludi A (1988) High-pressure NMR kinetics. Part 34. Variable-temperature and variable-pressure NMR kinetic study of solvent exchange on hexa-aqua-ruthenium(3+) and -(2+) and hexakis(acetonitrile)ruthenium(2+). *Inorg Chem* 27:873–879. <https://doi.org/10.1021/ic00278a025>
- Sakthivel A, Hijazi AK, Hanzlik M, Chiang AST, Kühn FE (2005a) Heterogenization of $[Cu(NCCH_3)_6][B(C_6F_5)_4]_2$ and its application in catalytic olefin aziridination. *Appl Catal A* 294:161–167. <https://doi.org/10.1016/j.apcata.2005.07.018>
- Sakthivel A, Hijazi AK, Yeong HY, Köhler K, Nuyken O, Kühn FE (2005b) Heterogenization of a manganese(ii) acetonitrile complex on AlMCM-41 and AlMCM-48 molecular sieves by ion exchange. *J Mater Chem* 15:4441–4445. <https://doi.org/10.1039/B508533K>
- Sakthivel A, Syukri S, Hijazi AK, Kühn FE (2006) Heterogenization of $[Cu(NCCH_3)_4][BF_4]_2$ on mesoporous AlMCM-41/AlMCM-48 and its application as cyclopropanation catalyst. *Catal Lett* 111:43–49. <https://doi.org/10.1007/s10562-006-0128-5>
- Shelke V, Patharkar SM, Shankarwar VR (2012) Synthesis, spectroscopic characterization and thermal studies of some rare earth metal complexes of unsymmetrical tetradentate Schiff base ligand. *Arabian J Chem* 5:501–507. <https://doi.org/10.1016/j.arabjc.2010.09.018>
- Shriver D, Shriver SA, Anderson SE (1965) Ligand field strength of the nitrogen end of cyanide and structures of cubic cyanide polymers. *Inorg Chem* 4:725–730. <https://doi.org/10.1021/ic50027a028>
- Singh K, Kumar Y, Puri P, Singh G (2012) Spectroscopic, thermal, and antimicrobial studies of Co(II), Ni(II), Cu(II), and Zn(II) complexes derived from bidentate ligands containing N and S donor atoms. *Bioinorg Chem Appl*. <https://doi.org/10.1155/2012/729708>
- Solomon VR, Haq W, Srivastava K, Puri SK, Katti SB (2007) Synthesis and antimalarial activity of side chain modified 4-aminoquinoline derivatives. *J Med Chem* 50:394–398. <https://doi.org/10.1021/jm061002i>
- Strauss SH (1993) The search for larger and more weakly coordinating anions. *Chem Rev* 93:927–942. <https://doi.org/10.1021/cr00019a005>
- Syukri S, Hijazi AK, Sakthivel A, Al-Hmaideen AI, Kühn FE (2007) Heterogenization of solvent-ligated copper(II) complexes on poly(4-vinylpyridine) for the catalytic cyclopropanation of olefins. *Inorg Chim Acta* 360:197–202. <https://doi.org/10.1016/j.ica.2006.07.104>
- Thomas RR, Sen A (1989) Acetonitrile complexes of selected transition metal cations. *Inorg Synth* 26:128–134. <https://doi.org/10.1002/9780470132579>

- Thomas RR, Chebolu V, Sen A (1986) Chemistry of weakly solvated lanthanide-metal cations. Synthesis, characterization, and catalytic chemistry of $[\text{Eu}(\text{CH}_3\text{CN})_3(\text{BF}_4)_3]_x$. *J Am Chem Soc* 108:4096–4103. <https://doi.org/10.1021/ja00274a039>
- Vierle M, Zhang Y, Herdtweck E, Bohnenpoll M, Nuyken O, Kühn FE (2003) Highly reactive polyisobutenes prepared with manganese(II) complexes as initiators. *Angew Chem Int Ed* 42:1307–1310. <https://doi.org/10.1002/anie.200390337>
- Vierle M, Zhang Y, Köhler K, Häßner C, Santos AM, Herdtweck E, Nuyken O, Kühn FE (2004) Solvent-ligated manganese(II) complexes for the homopolymerization of isobutene and the copolymerization of isobutene and isoprene. *Chem Eur J* 10:6323–6332. <https://doi.org/10.1002/chem.200400446>
- Wheeler OH, Gonzales D (1964) Oxidation of primary aromatic amines with manganese dioxide. *Tetrahedron* 20:189–193. [https://doi.org/10.1016/S0040-4020\(01\)93207-7](https://doi.org/10.1016/S0040-4020(01)93207-7)
- White RW, Emmons WD (1962) The chemistry of permaleic acid. *Tetrahedron* 17:31–34. [https://doi.org/10.1016/S0040-4020\(01\)99002-7](https://doi.org/10.1016/S0040-4020(01)99002-7)
- Zhao R, Tan C, Xie Y, Gao C, Liu H, Jiang Y (2011) One step synthesis of azo compounds from nitroaromatics and anilines. *Tetrahedron Lett* 52:3805–3809. <https://doi.org/10.1016/j.tetlet.2011.05.054>

Publisher's Note Springer Nature remains neutral with regard to jurisdictional claims in published maps and institutional affiliations.